

This document is confidential and is proprietary to the American Chemical Society and its authors. Do not copy or disclose without written permission. If you have received this item in error, notify the sender and delete all copies.

**Base-catalyzed Aryl-B(OH)₂ Protodeboronation Revisited:
from Concerted Proton-Transfer to Liberation of a Transient
Arylanion**

Journal:	<i>Journal of the American Chemical Society</i>
Manuscript ID	ja-2017-07444r.R1
Manuscript Type:	Article
Date Submitted by the Author:	n/a
Complete List of Authors:	Cox, Paul; University of Edinburgh Reid, Marc; University of Edinburgh Leach, Andrew; Liverpool John Moores University, School of Pharmacy and Biomolecular Sciences Campbell, Andrew; AstraZeneca, Pharmaceutical Technology and Development King, Edward; TgK Scientific Ltd Lloyd-Jones, Guy; University of Edinburgh, School of Chemistry

SCHOLARONE™
Manuscripts

Base-catalyzed Aryl-B(OH)₂ Protodeboronation Revisited: from Concerted Proton-Transfer to Liberation of a Transient Arylanion

Paul A. Cox,[†] Marc Reid,[†] Andrew G. Leach,[‡] Andrew D. Campbell,[§] Edward J. King,[&] and Guy C. Lloyd-Jones^{*,†}

[†] School of Chemistry, University of Edinburgh, Joseph Black Building, David Brewster Road, Edinburgh, EH9 3FJ, UK

[‡] School of Pharmacy and Biomolecular Sciences, Liverpool John Moores University, Byrom Street, Liverpool L3 3AF, UK

[§] AstraZeneca, Silk Road Business Park, Macclesfield, SK10 2NA, UK

[&] TgK Scientific Limited, 7 Long's Yard, St Margaret's Street, Bradford-on-Avon, BA15 1DH, UK

ABSTRACT: Pioneering studies by Kuivila, published more than 50 years ago, suggested *ipso*-protonation of the boronate as the mechanism for base-catalyzed protodeboronation of arylboronic acids. However, the study was limited to UV spectrophotometric analysis under acidic conditions, and the aqueous association constants (K_a) estimated. Using NMR, stopped-flow IR, and quench-flow techniques, the kinetics of base-catalyzed protodeboronation of 30 different arylboronic acids have now been determined at pH >13 in aqueous-dioxane at 70 °C. Included in the study are all twenty isomers of C₆H_nF_(5-n)B(OH)₂ with half-lives spanning nine orders of magnitude: <3 msec to 6.5 months. In combination with pH-rate profiles, pK_a , ΔS^\ddagger , KIEs (²H, ¹⁰B, ¹³C), linear free-energy relationships, and DFT, we identify a mechanistic regime involving unimolecular heterolysis of the boronate competing with concerted *ipso*-protonation / C-B cleavage. The relative Lewis acidities of arylboronic acids do not correlate with their protodeboronation rates, especially when *ortho*-substituents are present. Notably, 3,5-dinitrophenyl boronic acid is orders of magnitude more stable than tetra and penta-fluorophenyl boronic acids, but has a similar pK_a .

INTRODUCTION

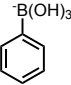
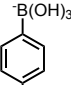
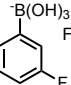
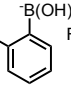
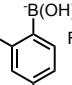
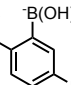
Boronic acids have a long history of application in the chemical sciences.¹ They provide conveniently-handled, or in situ generated² nucleophiles for a host of cross-coupling and substitution reactions.³ However, their application extends far wider than this, finding use for example as radical-precursors,⁴ Lewis acid catalysts,⁵ for aryl-deuteration,⁶ as traceless catalyst-directing groups,⁷ as chemo-sensors,⁸ as functional groups in materials,⁹ as gelators,¹⁰ self-healing polymers,¹¹ in ¹⁸F-labelling,¹² and in drug design.¹³

An understanding of the factors that control the stability of boronic acids can inform their more effective application. One of the primary decomposition pathways of arylboronic acids is protodeboronation;¹⁴ the conversion of Ar-B(OH)₂ to Ar-H. The process is generally an undesired one: reducing yields and increasing side-products.¹⁵ In some circumstances however, protodeboronation is productive.¹⁶ This includes for example the traceless removal of a B(OH)₂-blocking^{16a} or directing group,^{16b} in deborylative synthetic strategies,^{16c} or for the *in situ* purging of genotoxic¹⁷ arylboronic acid residues from Suzuki-Miyaura reactions. As a consequence, the acceleration of protodeboronation is a field of significant current interest.¹⁸

Mechanistic insight into the impact of aqueous base and acid on the rate of protodeboronation is particularly useful in the context of Suzuki-Miyaura cross-coupling.^{3ab} For basic heteroarylboronic acids, the effects can be complex and counter-intuitive.^{14m} In contrast, non-basic heteroaryl-, alkyl-, and vinyl-boronic acids, undergo simple acid- and base-catalyzed processes.^{14m} In seminal early studies, Kuivila^{14c-e} measured the rates of aqueous acidic protodeboronation (90

°C, pH range 2.0 to 6.7; UV-vis spectrophotometry) of a small series of mono-substituted arylboronic acids.^{14e} Kuivila deduced from this data that, in addition to an acid-catalyzed pathway involving the boronic acid, there is a mechanism involving the boronate ([ArB(OH)₃]⁻) generated in a pH-controlled equilibrium (K_a).¹⁹ The rates of protodeboronation could not be determined above pH 7, due to the appearance of strongly UV-absorbing side-products.^{14e} Nonetheless, the limiting reaction rates, estimated by extrapolation to pH > 13²⁰ ($k_{rel(est.)}$, Scheme 1) appeared to show that protodeboronation is retarded by a fluorine substituent at the *m*-position, and accelerated by a fluorine at the *o/p*-position. The greater acceleration by *o*-F was ascribed to electrostatic repulsion between B(OH)₃⁻ and F.

Scheme 1. Dichotomous effects of F-substituents on the relative rates²⁰ of aqueous protodeboronation of arylboronates.

							
$k_{rel(est.)}$	1.0	1.4	0.3	11	--	--	Kuivila
$k_{rel(obs)}$	1.0	1.4	0.98	243	616	1548	This work

However, the effects of fluorine substituents are dichotomous. Compare for example, phenyl, 4-F-, and 3-F-phenyl boronates, which have near-identical rates ($k_{rel(obs)}$, Scheme 1), to the analogous *o*-fluorinated series (2-F-, 2,4-F₂-, and 2,5-F₂-) in which the 4-F and 3-F substituents induce significant rate-acceleration. The origins of these effects are the subject of the work presented herein. We report kinetic data for the base-catalyzed protodeboronation of 30 arylboronic

acids, including all isomers of $C_6H_nF_{(5-n)}B(OH)_2$ ($n = 0$ to 5). Some of these species are many orders of magnitude more reactive than the notoriously unstable²¹ 2-pyridyl system ($t_{0.5} = 27$ sec, at $70^\circ C$, pH 7 in 50 % aq. dioxane).^{14m} In combination with thermodynamic reaction parameters, pH-rate profiles, pK_a -determination, computational analysis, the effect of counter-cation ($[ArB(OH)_3]^- [M]^+$), kinetic isotope-effects (2H , ^{10}B , ^{13}C), and linear free-energy relationships, a dual mechanistic regime is identified for arylboronic acid protodeboronation. The study shows that trihydroxyboronates generated from highly electron-deficient arylboronic acids under aqueous conditions are inherently unstable. Highly electron-deficient arylboronic acids have negligible susceptibility to acid-catalyzed protodeboronation, and their Lewis acidity is not directly related to their rates of protodeboronation under basic conditions.

RESULTS AND DISCUSSION

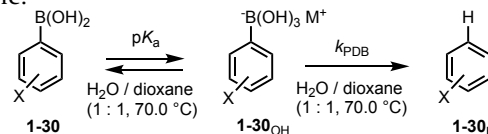
Electron-deficient and *ortho*-substituted arylboronic acids have considerable utility in cross-coupling,^{14i,22} as catalysts,⁵ and in sensors.⁸ Some of these species undergo rapid decomposition under basic conditions. For example, polyfluorophenyl boronic acids require specialized catalysts to be efficiently cross-coupled.^{14i,22} Data on the base-mediated protodeboronation of various classes of electron-deficient arylboronic acids and boronates are available from prior studies by Kuivila,^{14e} Fröhlich,^{14g} Cammidge,^{14h} Buchwald,¹⁴ⁱ Perrin,^{14j} and Adonin.^{14k} However, an holistic mechanistic analysis is limited by i) the restricted range of substrates for which comparable kinetic data has been reported, ii) the wide variations in conditions employed between studies, and iii) an absence of pH-rate profiling and pK_a data, in the majority of cases. Nonetheless, the above studies^{14e,14g-k} reveal that all 2,6-dihalogenated phenyl boronic acids are highly susceptible to protodeboronation when exposed to base.

1. Acquisition of Kinetic Dataset In order to study the mechanism of protodeboronation of electron-deficient arylboronic acids in more detail we selected 30 examples (1-30, Table 1) for kinetic analysis. The selection deliberately includes a number of examples that overlap with previous studies.^{14e,14h-j} Obtaining a coherent set of kinetic data across the whole series (1-30) required careful choice of reaction conditions and methodology. A 1 : 1 mixture of H_2O and dioxane at $70^\circ C$ (26.8 M H_2O - see SI) was found to give tractable boronic acid solubility across a wide range of pH and salt concentrations. These conditions also allow direct comparison of kinetic data for 1-30 with 16 heteroaromatic boronic acids, including the highly reactive 2-pyridyl and 5-thiazolyl species.^{14m}

Protodeboronation reactions of 1-30 were conducted at pH ≥ 13 , *vide infra*. Under these conditions, the reactant is exclusively in its boronate form and the resulting (pseudo) first-order decays (k_{obs}/s^{-1}) are pH-independent, without complication from self- or auto-catalysis.^{14m} Reactions were initiated by addition of a solution of strong base (excess KOH) to a solution of the boronic acid, and quenched, if required, by pH-drop (excess HCl). Automated flow techniques were employed for fast reactions, allowing thermostatted rapid-mixing of the various solutions. Aqueous-dioxane stock solutions of the boronic acids contained 10 mol% propionic or trifluoroacetic acid as combined internal NMR reference and stabilizer. The most reactive (27-30) required 110 mol% trifluoroacetic acid to avoid significant protodeboronation of the stock solution, prior to addition of the base at $70^\circ C$.

The wide scale of reactivity encountered for 1-30 required a range of techniques be applied for determination of the reaction kinetics. Slow reactions ($t_{0.5}$ days to months) were conducted in sealed quartz^{14m} NMR tubes at $70^\circ C$, and monitored periodically by 1H or ^{19}F NMR at $70^\circ C$. Reactions with intermediate rates ($t_{0.5}$ hours) were again set up in quartz NMR tubes at $70^\circ C$, but as a series, with manual pH-quenching of individual tubes at increasing time intervals, followed by analysis by $^1H/^{19}F$ NMR at ambient temperature. Fast reactions ($t_{0.5}$ seconds to minutes) were analyzed *in situ* at $70^\circ C$ using a stopped-flow ATR-FTIR device. Very fast reactions ($t_{0.5}$ milliseconds) were conducted by rapid quench-flow at $70^\circ C$, prior to off-line analysis by ^{19}F NMR.

Table 1. Aqueous association (pK_a) and protodeboronation (k_{PDB}) of arylboronates 1-30_{OH}, $70^\circ C$ in 1 : 1 H_2O / dioxane.

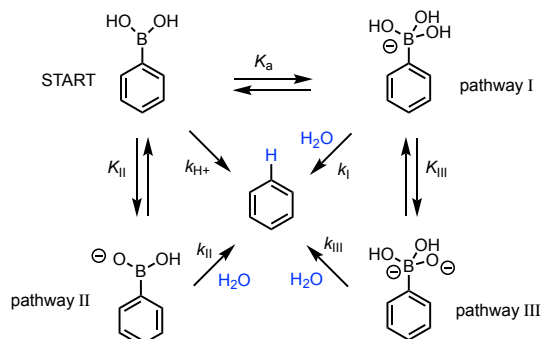


Substrate; X	pK_a	$\log k_{PDB}$	$\sim t_{0.5}$
1 3-F	10.46 ^a	-7.40	7 months
2 H (phenyl)	11.25 ^a	-7.39	6 months
3 4-F	10.97 ^a	-7.23	4 months
4 3,4-F ₂	10.34 ^a	-7.13	3 months
5 3,5-F ₂	9.78 ^a	-7.08	3 months
6 3-Cl	10.56 ^a	-6.85	8 weeks
7 3,5-(CF ₃) ₂	9.38 ^a	-6.81	7 weeks
8 4-Me	11.75 ^a	-6.80	7 weeks
9 3,4,5-F ₃	9.44 ^a	-6.77	7 weeks
10 4-MeO	11.78 ^a	-6.62	5 weeks
11 3,5-(NO ₂) ₂	7.91 ^a	-4.92	16 hours
12 2-F-4-MeO	10.78 ^a	-5.25	34 hours
13 2-F	10.14 ^a	-5.00	19 hours
14 2,4-F ₂	10.02 ^a	-4.60	8 hours
15 2,5-F ₂	9.34 ^a	-4.20	3 hours
16 2-F-4-CF ₃	9.04 ^a	-4.03	2 hours
17 2,3-F ₂	9.51 ^a	-3.92	2 hours
18 2,4,5-F ₃	9.00 ^a	-3.76	1 hour
19 2,3,4-F ₃	9.06 ^a	-3.53	39 mins
20 2-F-5-NO ₂	8.22 ^b	-3.10	15 mins
21 2,3,5-F ₃	8.47 ^a	-2.95	10 mins
22 2,3,4,5-F ₄	8.91 ^b	-2.41	3 mins
23 2,6-F ₂ -4-MeO	9.56 ^b	-1.01	7 sec
24 2,6-F ₂	9.15 ^b	-0.87	5 sec
25 2,4,6-F ₃	9.03 ^b	-0.26	1 sec
26 2,3,6-F ₃	8.66 ^b	0.47	235 msec
27 2,3,4,6-F ₄	8.39 ^b	1.02	66 msec
28 2,3,5,6-F ₄	7.97 ^b	1.79	11 msec
29 2,3,5,6-F ₄ -4-MeO	8.33 ^b	1.88	9 msec
30 2,3,4,5,6-F ₅	7.67 ^b	2.43	2.6 msec

^a Measured by ^{11}B NMR pH titration. ^b Estimated by correlation of the pH-dependency of the protodeboronation rate, using $k_{obs(OH)} = k_{PDB} / \{1 + 10^{(pK_a - pH)}\}$, see SI.

2. Correlation of kinetics with pH In his pioneering studies on protodeboronation, Kuivila used pH-extrapolation²⁰ to predict the Hammett correlation for reaction under strongly basic conditions - despite being unable to directly measure this. On the basis of the negative gradient ($\rho = -2.3$)²³ found for the correlation, he proposed that protodeboronation involves *ipso*-protonation of an arylboronate intermediate by water (pathway I, Scheme 2).^{14e} Two alternative pathways (II, III) have been proposed by Fröhn,^{14g} and by Perrin,^{14j} to account for the rapid protodeboronation of *ortho*-halogenated systems. Both mechanisms invoke an *ortho*-halogen-induced Brønsted acidity in the B-OH functionality, in either the boronic acid (pathway II) or the boronate (pathway III).

Scheme 2. Mechanisms I-III, previously proposed for base-catalyzed protodeboronation of arylboronic acids.



In our earlier study on heteroaromatic boronic acids, we demonstrated that a detailed pH-rate profile (pH 1-13) allows correlation of speciation, $[H]^+/[OH]^-$ concentration, and rate, with changes in mechanism.^{14m} Indeed, this technique allowed us to deduce that the kinetically-unique Perrin mechanism^{14j} (III) is responsible for the rapid protodeboronation of 4-pyrazolyl- and 3,5-dimethyl-4-isoxazolyl boronates under strongly basic conditions ($pH \geq pK_a + 2$).^{14m}

A pH-rate analysis was thus conducted for 2,6-difluorophenyl boronic acid (**24**, $pK_a = 9.15$), one of the faster reacting arylboronic acids in the series **1-30**. The rate of its protodeboronation increases >6 orders of magnitude as the buffered-pH is raised from 1 to 13, Figure 1A. Mechanisms proceeding *via* a mono-anion, generated by association of OH^- (pathway I) or by deprotonation of B-OH (pathway II) are kinetically indistinguishable in terms of pH-dependency: ($k_{obs(OH)} = k_{PDB}/\{1+10^{(pK_a-pH)}\}$). For **24** ($pK_a = 9.15$) this function predicts a linear correlation (gradient +1) of $\log_{10}k_{obs}$ versus pH, at pH values below 7.15 ($pK_a - 2$). At pH values above this, the gradient progressively attenuates, becoming zero, i.e. the rate is pH-independent, when $pH \geq 11.15$; ($pK_a + 2$). This simple model correlates well with the data, see dashed blue line in Figure 1A. There is no evidence for any significant acid-catalysis ($k_{obs(H^+)} = k_H/[10^{pH}(1+10^{(pH-pK_a)})}$), or bimolecular contributions from self/auto-catalysis in the pH region close to the pK_a .²⁴

Mechanism III is kinetically distinct ($k_{obs} = k'_{III}(10^{(pH-pK_w)})/\{1+10^{(pK_a-pH)}\}$)²⁵ from I and II, even when $pK_a = pK_{III}$, (see red dashed lines in Figure 1A). An exception to this is if two mechanisms are operating in parallel, with $k_{PDB} = k_{III}$, and $pK_a = pK_{III}$. To test this possibility, the rate of protodeboronation²⁶ of **24** was determined as a function of initial $[KOH]/[24]$ ratio. There is a clear 'saturation' in hydroxide when $[KOH]/[24] \approx 1.0$, Figure 1B. Mechanisms proceeding *via* equilibrium of the boronic acid with the mono-anion

(boronate) reach a rate-maximum when the initial ratio is close to unity. Mechanism III, which proceeds via a formally dianionic pathway, requires super-stoichiometric KOH to reach rate-saturation (dashed red line). The same hydroxide-dependence (dashed blue line) was observed at 21 °C. Pentafluorophenyl boronic acid (**30**), the most reactive substrate in the series, behaved analogously (See SI).

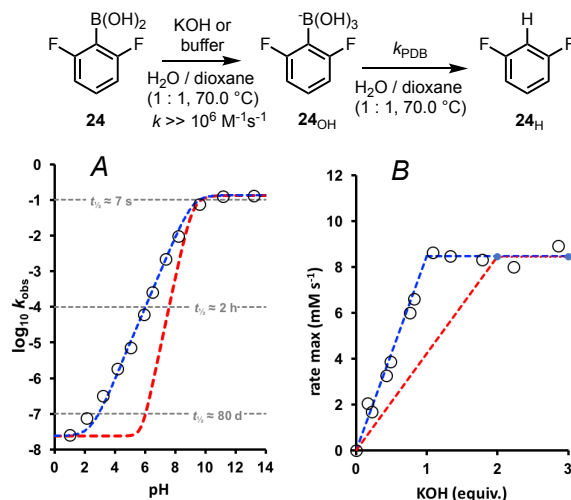


Figure 1. Protodeboronation of 2,6-difluorophenyl boronic acid (**24**, 51 mM), 70 °C. Circles experimental data. Graph A: pH- $\log k_{obs}$ profile; buffered pH. Blue line: mono-anionic mechanisms (e.g. I/II/IV) where $k_{obs} = k_{PDB}/\{1+10^{(pK_a-pH)}\} + k_b$; $pK_a = 9.15$, $k_{PDB} = 0.135 \text{ s}^{-1}$, and $k_b = 3 \times 10^{-8} \text{ s}^{-1}$. The latter is a very slow uncatalyzed process.^{14e,14m} Red line: mechanism III where ($k_{obs} = k'_{III}(10^{(pH-pK_w)})/\{1+10^{(pK_a-pH)}\} + k_b$); $pK_a = pK_{III}$; $k'_{III} = 0.135 \text{ s}^{-1}$; $k_b = 3 \times 10^{-8} \text{ s}^{-1}$. Graph B: rate dependence on KOH stoichiometry.

3. Dichotomous LFER As noted above, the disparate effects of electronegative substituents (Scheme 1) were interpreted by Kuivila within the context of Mechanism I: electrostatic repulsion (*ortho*-X) accelerates protonolysis of the boronate, whereas inductive effects (*meta/para*-X) attenuate it.^{14e} Since the electronic influence of sterically unencumbered substituents should be independent, i.e. their Hammett σ -values additive,²⁷ predictable effects should arise from *ortho*- versus *meta/para*- multiple substitutions. This aspect was tested by LFER correlation of three sub-groups (see dashed lines in Table 1): those with no *ortho*-substituent (**1-11**, group 1), those with a single *ortho*-fluoro substituent (**12-22**, group 2) and those with two *ortho*-fluoro substituents (**23-30**, group 3).

Isolating the three sub-groups, means that if the same mechanism (I or II) is operative throughout, each group should show a similar correlation (ρ) to that predicted by Kuivila ($\rho = -2.3$) for the mono-substituted *m/p*-X-C₆H₄-B(OH)₂ series.^{14e} However, as shown in Figure 2, sub-groups 2 and 3 both have a positive gradient ($\rho = +4$), whereas sub-group 1 has a flat, marginally concave profile. The 3,5-dinitro substituted boronic acid **11** ($\sigma = 1.42$) is an evident outlier in sub-group 1, undergoing protodeboronation around two orders of magnitude faster than **1-10**. The similar positive-gradient correlations in sub-groups 2 and 3 shows that an additional *ortho*-fluoro substituent accelerates the rate by approximately 2.5×10^4 . Further inspection of sub-groups 2 and 3 shows that MeO, CF₃ and NO₂ substituents (blue squares) cause consistent small deviations from the trend exhibited by the

solely fluorinated systems (red circles, Figure 2). The directions of displacement are indicative that standard sigma values overestimate the resonance contribution by MeO (**12**, **23**, **29**) and underestimate the inductive effects of CF₃ (**16**) and NO₂ (**20**) for this particular mechanism.

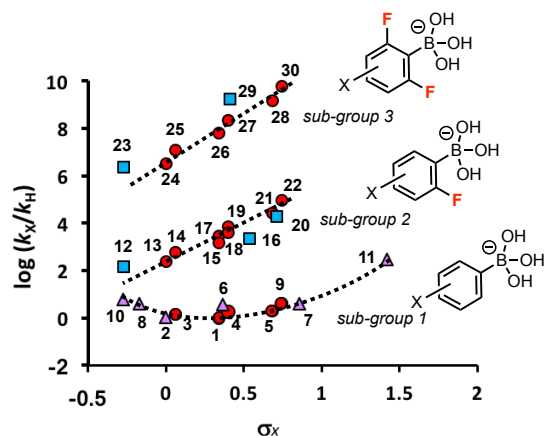


Figure 2. Hammett analyses of protodeboronation of arylboronic acids **1-11** (sub-group 1); **12-22** (sub-group 2); and **23-30** (sub-group 3); 50 mM RB(OH)₂, 1:1 H₂O/dioxane, 70 °C, pH > pK_a + 2. Dashed lines through data are solely a guide to the eye. Red circles: substrates with fluorine substituents only. Blue squares: substrates with additional non-fluorine substituents. Purple triangles: non-fluorinated substrates.

To refine the analysis of **1-30**, a Swain-Lupton correlation was constructed, Figure 3, combining all of the above observations. A field-dominated parameterization ($0.69 F + 0.31 R$) was applied to reduce the resonance contribution of MeO and F, and to unify the three sub-groups, an empirical value of $\sigma^{o-F} = 1.24$ included for each *ortho*-F substituent. The resulting correlation has two regions; that above $\sigma^{SL} \geq 0.7$ is mechanistically continuous ($\rho^{SL} = +3.4$), and mechanistically distinct from the region $\sigma^{SL} \leq 0.7$.

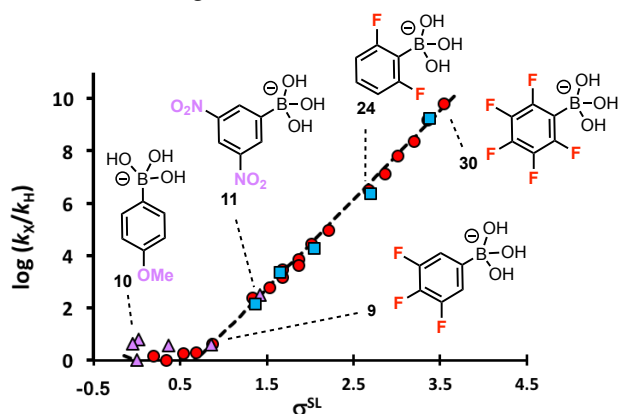


Figure 3. LFER for the protodeboronation of the boronate form of arylboronic acids **1-30**, using a modified Swain-Lupton parameter, $\sigma^{SL} = [0.69 F + 0.31 R + n(\sigma^{o-F})]$; $\sigma^{o-F} = 1.24$; n = number of *ortho*-F. Symbol coding: see Figure 2.

The region $\sigma^{SL} \leq 0.7$ predominantly contains substrates studied by Kuivila as part of the mono-substituted *m/p*-X-C₆H₄-B(OH)₂ series, and for which Mechanism I was proposed.^{14c} Importantly, 3,4,5-trifluorophenyl (**9**, $\sigma^{SL} = 0.84$) and 3,5-dinitro-phenyl boronic acid (**11**, $\sigma^{SL} = 1.42$) lie within and upon the correlation for the upper region ($\sigma^{SL} \geq 0.7$). This indicates that it is the combined electronic-effect (predomi-

nantly inductive) of the substituents that controls which of two distinct mechanistic pathways is followed, *not* the presence of halogens, or *ortho* substituents.^{14j}

4. Lewis-Acidity of ArB(OH)₂ Species Polyfluorinated arylboronic acids have been proposed to possess enhanced Brønsted acidity (II, Scheme 2), providing an alternative^{14b} pathway to the Kuivila mechanism (I).^{14c} Although these mechanisms (I and II, Scheme 2) are kinetically indistinguishable, *vide supra*, trigonal / tetrahedral boron centres related by equilibrium have characteristic differences in their ¹¹B NMR chemical shift and line-width.²⁹ For boronic acids in aqueous media, rapid intermolecular exchange ($\sim 10^6$ M⁻¹s⁻¹) of hydroxyl-ligands between boronic- and boronate-centres results in a single time-average population-weighted ¹¹B NMR signal, with $\Delta\delta_B$ tet→trig ≈ 30 ppm.²⁹ The majority of boronic acids **1-30** proved stable enough at 70 °C for ¹¹B{¹H} NMR pH-titration studies. The 20 examples (**1-19**, **21**) that could be analysed in detail (see SI) span both of the mechanistic regimes identified by the Swain-Lupton analysis (above and below $\sigma^{SL} = 0.7$, Figure 3). All examples displayed time-average ¹¹B NMR chemical shifts and line-widths characteristic of generation of a Lewis-acid adduct, i.e. a tetrahedral boronate, [ArB(OH)₃]⁻, for which K_a, Table 1, was determined using the Henderson-Hasselbalch relationship. Since the rate of protodeboronation (k_{obs}) directly correlates with the boronate population, K_a, Figure 1A, there is no evidence for any significant contribution by mechanism II under these highly aqueous conditions.³⁰

Analysis of the entire dataset (Table 1) shows that the impact of *ortho*-F substitution on the Lewis-acidity of the boronic acid (K_a) is much less marked than it is on the rate of decomposition (k_{obs}) of the corresponding boronate. The Lewis acidity can be correlated using regular Hammett σ -values for *m,p*-substituents, again normalizing the three groups of boronic acids by inclusion of an empirical value²⁸ ($\sigma^{o-F} = 0.45$) for each *ortho*-F substituent, Figure 4.³¹ Although 1 : 1 H₂O / dioxane increases the pK_a of aryl boronic acids by approximately 2 units relative to that measured in water,^{5j,14m,29,31} the relative Lewis acidities are not significantly changed: $\rho = 2.4$ versus $\rho = 2.1$ in H₂O at ambient temperature.³¹

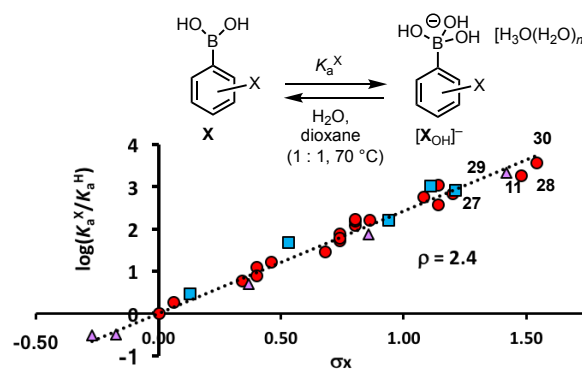
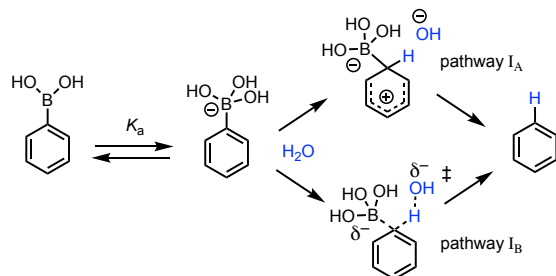


Figure 4. Modified Hammett correlation of the aqueous association constant (K_a) to generate [ArB(OH)₃]⁻ [H₃O(H₂O)_n]⁺ in 1:1 H₂O/dioxane at 70 °C, for arylboronic acids **1-30**, where $\sigma = [\sigma_X + n(\sigma^{o-F})]$; $\sigma^{o-F} = 0.45$; n = number of *ortho*-F. Symbol coding: see Figure 2.

5. Protodeboronation via Mechanism (I) Of the thirty arylboronic acids studied, eight (**1-6**, **8** and **10**) are in the $\sigma^{SL} \leq 0.7$ region of the Swain-Lupton analysis, Figure 3, and are

mechanistically distinct from those where $\sigma^{\text{SL}} \geq 0.7$. Six of these (**1-3**, **6**, **8** and **10**) have been previously studied by Kuivila (at 90 °C in malonate-buffered water, pH 6.7) who proposed an aromatic electrophilic substitution pathway via *ipso*-protonation of the arylboronate by H₂O (Mechanism I_A, Scheme 3).^{14e} However, key in the analysis was a series of data that were determined under acidic conditions (pH 6.7, 25 °C, uncorrected) and then normalized for LFER correlation ($\rho = -2.3$) by calculation of boronate population using estimated K_a values.^{14e,19,20}

Scheme 3. Step-wise (I_A)^{14e} and concerted (I_B) mechanisms for base-catalyzed arylboronic acid protodeboronation.



By conducting reactions at high pH, we have directly determined the rates of protodeboronation of the arylboronate. The data for boronates **1-3**_{OH}, **6**_{OH}, **8**_{OH} and **10**_{OH} ($\sigma^{\text{SL}} \leq 0.7$, Figure 3) shows that the rate (k_{obs}) is less sensitive to the substituents ($|\rho| \leq 1$) than previously estimated by Kuivila.^{14e} This aspect was explored computationally. A transition state (TS) could not be located (DFT, Mo6L/6-311++G**) for a step-wise protonation mechanism (pathway I_A). Instead, the lowest barrier pathway found for protodeboronation of **1-3**_{OH} and *p*-anisylboronate **10**_{OH}, bypasses generation of a Wheland intermediate^{14e} to directly liberate the arene protodeboronation product (Ar-H). The TS for this pathway (I_B) is analogous to that previously found for the protodeboronation of 3-thienylboronate.^{14m} At the TS, Figure 5, the *p*-anisyl ring is midpoint in its translation from the Lewis acid (B(OH)₃) to the Brønsted acid (OH), the process being initiated by development of a network of H-bonds between incoming water and the trihydroxyboronate.

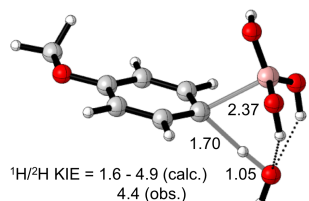


Figure 5. Transition state (Mo6L/6-311++G**) for protodeboronation of *p*-anisylboronate (**10**_{OH}) via Mechanism I_B (Scheme 3), where proton transfer to the *ipso*-carbon is concerted with C-B cleavage.

A primary kinetic isotope effect (PKIE) was found to attend the rate-limiting proton transfer (Figure 5). The absolute rate-differential ($k_{\text{H}}/k_{\text{D}} = 4.4$; determined in 1 : 1 D₂O / dioxane) was identical to the product partitioning factor (Ar-H/Ar-D = 4.4) obtained in 1 : 1 L₂O / dioxane (L = H / D; 50/50). The computed PKIE for the TS in Figure 5 is 1.56 (including the Wigner correction for tunnelling)³⁵ but this is increased as explicit solvent molecules are included and becomes 2.07 when one solvating water acts as a hydrogen

bond donor to the first water molecule and 4.87 when a second solvating water is added in the same role (these are increased further when the PCM parameters for water are used). Such sensitivity to structural changes for proton transfer KIEs was recently discussed by Aziz and Singleton.³⁶ Overall, we conclude that concerted mechanism I_B (Scheme 3, Figure 5) best describes the base-catalyzed protodeboronation of electron rich, neutral and mildly electron-deficient arylboronic acids ($\sigma^{\text{SL}} \leq 0.7$).

6. Protodeboronation via Mechanism (IV) The remaining 22 boronic acids (**7**, **9**, **11-30**) are distinct from those where $\sigma^{\text{SL}} \leq 0.7$ (Figure 3) which react via pathway I_B (Scheme 3). The change in gradient ($\rho^{\text{SL}} = +3.4$) is indicative of the onset of a new process: mechanism IV. The fast-reacting 2,6-difluorophenyl boronic acid (**24**; $\sigma^{\text{SL}} = 2.67$, $t_{0.5} \sim 5$ sec.) was selected for more detailed study. The pH-rate profile (Figure 1A), and ¹¹B NMR analysis, shows that mechanism IV also involves the arylboronate, **24**_{OH}. This species is thus a common intermediate to pathways I_B and IV, with branching dictated by aryl electron-demand. The kinetics require (pseudo) first-order branching from the arylboronate, and this essentially limits possibilities to associative (bimolecular, H₂O, I_B), dissociative or rearrangement (unimolecular) mechanisms.

Activation parameters for protodeboronation of **24**_{OH} (determined between 22.6 and 70.4 °C, using SF-ATR-FTIR, see SI) indicates an increase in entropy ($\Delta S^\ddagger = +6.2$ kcal.mol⁻¹K⁻¹) at the TS, weighing against associative or rearrangement processes. Further studies elucidated that the stability of arylboronate **24**_{OH} is mildly affected by the identity of the counter-cation (Figure 6). The Li⁺ boronate is the most stable in the series.³⁷ H-bonding interactions between water coordinated to M⁺ and the triskelion hydroxyl groups of the boronate are evident in the crystal structure of [10_{OH}][Na(H₂O)₆], reported by Cammidge.³⁸ Such interactions would serve to stabilize the boronate by partial dispersion of the negative charge into the solvation sphere around the counter-cation.

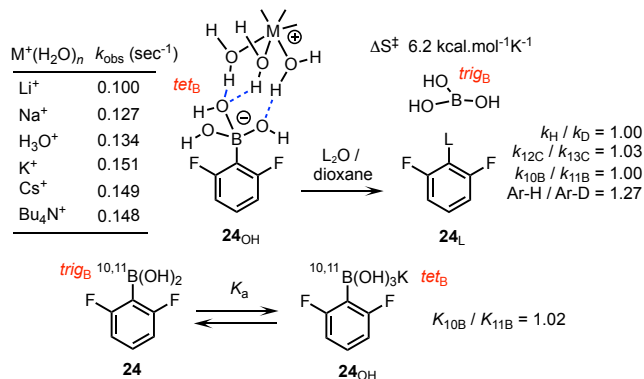


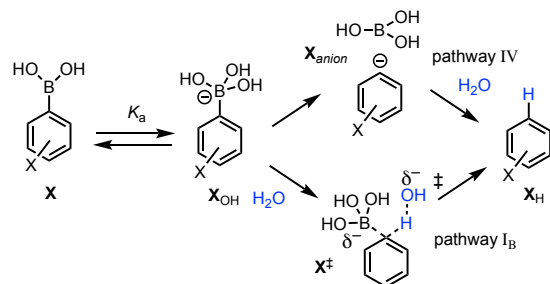
Figure 6. Protodeboronation of 2,6-difluorophenyl boronate ([**24**_{OH}]⁺K⁺). Kinetics for M⁺-variation determined at 70 °C; KIEs and EIEs determined at 27°C by natural abundance ¹³C, and by ²H/¹¹B/¹⁰B labelling; see SI.

In contrast to pathway I_B, the rate of protodeboronation of **24**_{OH} in 1 : 1 L₂O / dioxane was independent of the D/H ratio ($k_{\text{H}}/k_{\text{D}} = 1.00$); i.e. proton transfer is not rate-limiting. However, the product partitioning factor for **24**_{OH} is not unity, (Ar-H/Ar-D = 1.26; ten L₂O combinations; statistically-

corrected).³⁹ Elegant work by Perrin has shown that aqueous protonation of a nascent and genuinely *naked* arylanion, generated by barrier-less iodide-trapping of a *p*-benzyl diradical, proceeds with a low PKIE ($k_H/k_D = 1.2 \pm 0.1$; 55 °C) in an early transition state.⁴⁰ The partitioning factors (Ar-H/Ar-D) for protodeboronation of **24**_{OH}, **25**_{OH}, **26**_{OH}, **27**_{OH}, **28**_{OH} and **30**_{OH} in 1:1 L₂O / dioxane at 21 °C were all of a similar magnitude (average $k_H/k_D = 1.26 \pm 0.05$).

Heavy atom KIEs for the protodeboronation of 2,6-difluorophenyl boronate (**24**_{OH}) were also informative. A normal primary carbon-KIE ($k^{12}_C/k^{13}_C = 1.03$) was detected using Kwan and Jacobsen's DEPT modification of the Singleton ¹³C NMR technique.⁴¹ In contrast, the *net* ¹⁰B/¹¹B KIE, estimated by double-labelling^{2b} (²H, ¹⁰B, ¹¹B, see SI) is unity ($k^{10}_B/k^{11}_B \approx 1.00$). However, a large *inverse* KIE is known to accompany tetrahedral to trigonal reorganization at boron.⁴² Indeed, a significant *equilibrium* isotope effect ($K^{10}_B/K^{11}_B = 1.02$) was found for interconversion of **24** and **24**_{OH}, using double-labelling^{2b} in combination with Perrin's ¹⁹F NMR technique.⁴³ This then suggests that a normal boron-PKIE arising from C-B cleavage during protodeboronation of **24**_{OH} will be offset by an accompanying inverse KIE arising from tetrahedral to trigonal geometry change at boron.

Scheme 4. Substituent-controlled (X) branching of base-catalyzed arylboronic acid protodeboronation via dissociative (IV) versus concerted (I_B) protonolysis mechanisms.



Overall then, the experimental data for protodeboronation of **24**_{OH}, Figure 6, suggest that unimolecular heterolysis (mechanism IV, Scheme 4) of the aryl-boronate to generate boric acid is the rate-limiting event for boronates that lie in the $\sigma_{SL} \geq 0.7$ region of Figure 3. The lowest barrier found by DFT (Mo6L/6-311++G**) for protodeboronation of **24**_{OH} was C-B heterolysis (Figure 7) rather than concerted proton transfer from water (I_B) ($\Delta\Delta G^\ddagger = 2.0$ kcal mol⁻¹). Perrin has shown that the aqueous protonation of a naked arylanion is much faster than its combination with the counter-ion, i.e. M⁺, to generate Ar-M.⁴⁰ Rapid protonation accounts for the absence of benzyne products when there is a nucleofuge (e.g. Br)^{14j} adjacent to the boronate.⁴⁴

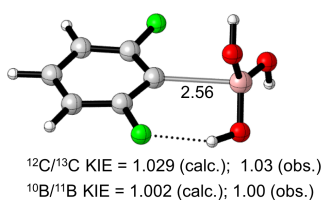


Figure 7. Transition state (Mo6L/6-311++G**) for heterolysis of 2,6-difluorophenylboronate (**24**_{OH}) via Mechanism IV.

7. Analysis of Branching (I_B / IV) Two mechanisms (I_B / IV) account for the kinetics of base-catalyzed protode-

boronation of all thirty arylboronic acids studied (**1-30**) herein. The factors dictating transit via one mechanism or the other were explored computationally. The relative reaction rates for mechanism IV can be rationalized on the basis of the intrinsic energy differences (ΔE) calculated for the unimolecular fragmentation of the arylboronate, Figure 8.

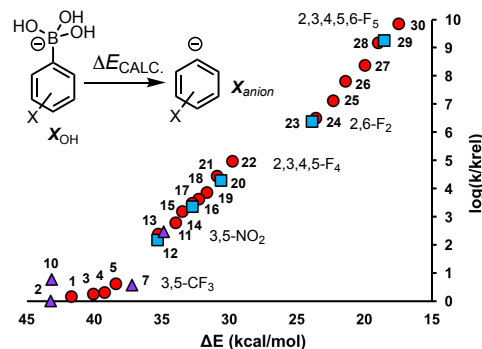


Figure 8. Rates of protodeboronation (y-axis) as a function of electronic energy (ΔE) for arylboronate heterolysis to generate an aryl carbanion (x-axis). See SI for full details. Symbol coding: see Figure 2.

Similar conclusions were derived from relative C-B bond orders using Wiberg Bond Indices⁴⁵ and from potential energy surface scans of C-B bond length, see SI. In the latter, the stepwise increase in ΔE en route to the aryl anion was lower in the substrates with greatest k_{obs} . DFT transition states³² (Mo6L/6-311++G**) were then calculated for mechanisms I_B and IV, for all 20 isomers of C₆H_nF_(5-n)B(OH)₂ ($n = 0$ to 5). The activation barriers (ΔG^\ddagger) suggests the two mechanisms become isoenergetic at $\Delta G^\ddagger = 22.2$ kcalmol⁻¹ ($\sim t_{0.5}$ 12 sec at 70 °C). Whilst the analysis overestimates the σ_{SL} value (1.6) for the crossing point, Figure 9, the general trend for transition from pathway I_B to IV as the net inductive effect of substituents is raised, is satisfactorily predicted.

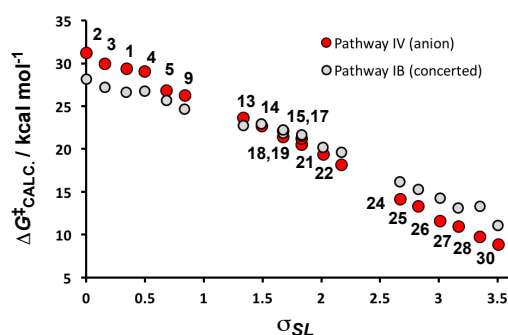


Figure 9. DFT transition state energies (Mo6L/6-311++G**); y-axis) versus augmented Swain-Lupton parameter (x-axis) for all 20 isomers of [C₆H_nF_(5-n)B(OH)₃]⁻ ($n = 0$ to 5) undergoing protodeboronation via pathways I_B / IV (see Scheme 4). $\sigma_{SL} = [0.69 F + 0.31 R + x(\sigma^{oF})]$; $\sigma^{oF} = 1.24$; x = number of *ortho*-F.

8. Anion stabilization through *ortho*-fluoro substitution

The above analysis provides experimental and computational evidence for a transition from mechanism I_B to mechanism IV, for specific classes of substrate. Mechanism IV involves generation of a transient naked arylanion.⁴⁶ Based on the differences in empirical values included in the Swain-Lupton correlations of k_{obs} (Figure 3, $\sigma^{oF} = 1.24$) and pK_a (Figure 4; $\sigma^{oF} = 0.45$) *ortho*-fluoro substituents are especially efficient at facilitating *ipso* arylanion generation. The origins of this

effect were examined through natural bond orbital (NBO) analysis⁴⁷ (Mo6L/6-311+G(d,p)) of the phenyl and 2,6-difluorophenyl anions (**2_{anion}** and **24_{anion}**). Delocalization of negative charge into the adjacent C(2)-C(3) and C(6)-C(5) antibonding orbitals ($n \rightarrow \sigma^*$), affords some stabilization of the anions. However, the major difference between the systems stems from the extent of $n \rightarrow \sigma^*$ delocalization into C(2)-F and C(6)-F, and the accompanying increase in the *s*-character at C(1), Figure 10. The additional stabilization energy provided by C(2,6)-F $n \rightarrow \sigma^*$ delocalization is around 7 kcal mol⁻¹ per C-F, more than accounting for the 2×10^5 rate-differential in their rates of protodeboronation.

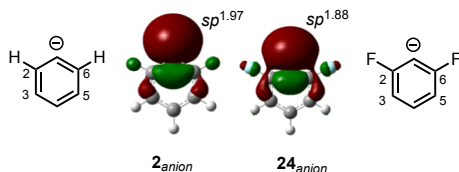


Figure 10. NLMO analyses^{47b} of arylanions **2_{anion}** and **24_{anion}** that would be generated by C-B heterolysis of boronates **2OH** and **24OH**. See SI for full details.

CONCLUSIONS

The mechanism of base-catalyzed protodeboronation of simple arylboronic acids, first established in 1963,^{14c} has been re-examined. With the benefits of modern instrumentation (NMR, stopped-flow IR, and rapid-quench flow) the reaction kinetics have been determined at high pH, where the boronic acid is exclusively in its boronate form, and maximum rate is achieved. The study has also substantially expanded the range of arylboronic acids for which protodeboronation kinetics have been determined, including highly electron-deficient polyfluorinated systems.

Kinetic, isotopic and computational data show that the mechanism originally proposed by Kuivila,^{14c} involving rate-limiting *ipso*-protonation by water, is valid for the base-catalyzed protodeboronation of arylboronic acids where the combined electron-demand of the substituents is below a critical point ($\sigma_{SL} \leq 0.7$, Figure 3). However, a concerted mechanism (**I_B**, Scheme 3) is now favoured over a step-wise

one (**I_A**).⁴⁸ Concerted proton-delivery to *ipso*-carbon is also mediated by $\text{ArB}(\text{OH})_2$ and $\text{B}(\text{OH})_3$, resulting in self/auto-catalysis when the pH is sufficiently close to the pK_a of the boronic acid.^{14m}

When the combined electron-demand of the substituents is raised above a critical point ($\sigma_{SL} \geq 0.7$, Figure 3) mechanism IV, involving unimolecular C-B cleavage, becomes kinetically competitive over pathway **I_B**. This dissociative process, which formally proceeds via liberation of an aryl anion, was also considered by Kuivila,^{14c} but discounted in favor of mechanism **I_A** on the basis of the Hammett correlation ($\rho = -2.3$) for a *m/p*-X-C₆H₄-B(OH)₂ series,²³ using estimated k_{PDB} values.⁴⁹

We have previously studied the protodeboronation of heteroaromatic systems.^{14m} A key mechanistic feature in those that undergo rapid protodeboronation, is a fragmentation reaction in which there is intramolecular stabilization of departing $\text{B}(\text{OH})_3$ during the C-B cleavage event. For the 2-pyridyl system this stabilization is provided by hydrogen bonding with the positively charged NH (see Figure 11). However, other stabilizing interactions, involving highly polarized CH and NH bonds, and anti-bonding orbitals in the heterocycle, are also found.^{14m} Mechanism IV, operates in a manner analogous to these processes, requiring an ability of the aryl ring to transiently accommodate the negative charge arising from fragmentation, prior to rapid intermolecular protonation, and for *ortho*-halogenated systems, intramolecular stabilization of $\text{B}(\text{OH})_3$ during C-B cleavage.

Perhaps surprisingly, with appropriate substituents, this process (IV) can be significantly more effective than in even the notorious 2-pyridyl system. Consideration of all possible isomers of C₆H_nF_(5-n)B(OH)₂ exemplifies the effect: the half-lives range from 6.5 months ($n = 1$, *meta*) to 2.6 msec ($n = 5$); a rate differential of 6.7×10^9 . *Ortho*-halogenated arylboronic acids undergo very fast protodeboronation^{14b-k} (mechanism IV, Figure 11) predominantly because the *ortho*-halogen is able to accommodate an *ipso*-aryl carbanion⁵⁰ by way of $n \rightarrow \sigma^*$ delocalization, and accompanying rehybridization with increased *s*-character at C(1), Figure 10. The change in mechanism from rate-limiting proton-delivery (**I_B**) to a dissociative one means that there is no significant self/auto-catalysis.^{14m}

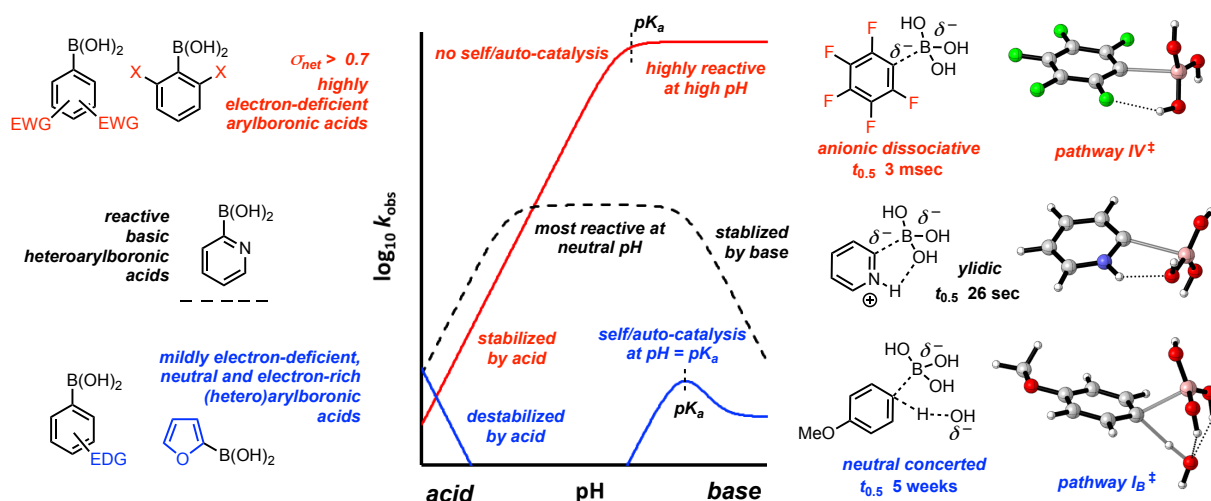


Figure 11. Pathways for arylboronic acid protodeboronation and associated effects of pH on rate. Half-lives for reaction in 1 : 1 dioxane water at 70 °C, at pH > 13 (C₆H₅ / C₆F₅) or at pH 7 (pyridyl). For details of self-catalysis and auto-catalysis, and mechanisms of protodeboronation of heteroarylboronic acids, see reference^{14m}.

However, some additional rather subtle and more-remote effects are also evident. For example, comparison of the rates of protodeboronation of **23/24** and **28/29** (Table 1) shows that *p*-MeO acts as a mild electron-donating group in **23**, but as a mild electron-withdrawing group in **29**. The restriction of C_{Ar}-OMe conformations by the adjacent F-substituents in **29**, results in less effective conjugation of OMe to the aromatic ring, as compared to **23**, and a higher field (*F*) effect. Comparison of the impact of aryl substituents on the Lewis-acidity versus stability of the boronic acid (Figures 4 and 3, respectively) is also instructive. 3,5-Dinitrophenyl boronic acid (**11**) is only marginally less Lewis-acidic ($\Delta pK_a = 0.24$) than pentafluorophenyl boronic acid (**30**),⁵⁰ but undergoes protodeboronation 7 orders of magnitude more slowly. This substantial disparity arises from the differing requirements of reduced π -delocalization for Lewis acidity and increased σ -delocalization for protodeboronation (via IV). This is reflected in the large field (*F*) contribution in the Swain Lupton analysis (Figure 3) and the differing impacts of *ortho*-F substitution for protodeboronation ($\sigma^{o-F} = +1.24$) versus Lewis-acidity ($\sigma^{o-F} = +0.45$). The marked stability of 3,5-dinitrophenylboronic acid **11** to protodeboronation may make it of considerable use as a Lewis acid catalyst.⁵ It is also of note that there is no significant acid-catalyzed protodeboronation for any of the highly electron-deficient arylboronic acids studied herein. This reinforces the conclusion that reactions that can tolerate or exploit lower pH conditions will be valuable vehicles for synthetic application of polyfluorophenyl and other highly electron-deficient arylboronic acids.^{22,51}

ASSOCIATED CONTENT

Supporting Information

Supporting Information: Additional discussion, experimental procedures, further kinetic data and analysis, full simulation fittings, characterization data and NMR spectra. This material is available free of charge via the Internet at <http://pubs.acs.org>.

AUTHOR INFORMATION

Corresponding Author

Guy.lloyd-jones@ed.ac.uk

Notes

PAC and MR contributed equally to this work.

Funding Sources

The research leading to these results has received funding from the European Research Council under the European Union's Seventh Framework Programme (FP7/2007-2013) / ERC grant agreement n° [340163]. AstraZeneca and the EPSRC provided an iCASE award (PC); the Carnegie Trust provided a collaborative research grant (MR).

ACKNOWLEDGMENT

We thank Dr Ruth Dooley (Edinburgh) for assistance with pulse calibrations and acquisition of ¹³C NMR DEPT spectra, and Prof Darren Dixon (Oxford) for discussion regarding the anomalous behavior of electron-deficient arylboronic acids.

REFERENCES

- (1) Hall, D. In *Boronic acids: preparation and applications in organic synthesis, medicine and materials (vols 1 and 2)*, second edition; Hall, D. (Ed.); Wiley VCH, Weinheim, Germany, 2011.
- (2) (a) Molander, G. A.; *J. Org. Chem.* **2015**, *80*, 7837–7848; (b) Gonzalez, J. A.; Ogba, O. M.; Morehouse, G. F.; Rosson, N.; Houk, K. N.; Leach, A. G.; Cheong, P. H. Y.; Burke, M. D.; Lloyd-Jones, G. C. *Nat Chem* **2016**, *8*, 1067–1075; (c) Iwade, N.; Sugimoto, M. *J. Am. Chem. Soc.* **2010**, *132*, 2548–2549.
- (3) Suzuki-Miyaura coupling is the classic application, ((a) Miyaura, N.; Yamada K.; Suzuki, A. *Tetrahedron Lett.* **1979**, *20*, 3437–3440; for a review see (b) Lennox, A. J. J.; Lloyd-Jones, G. C. *Chem. Soc. Rev.* **2014**, *43*, 412–433). Some selected examples of other important processes are oxidative Heck reactions ((c) Cho, C. S.; Uemura, S. *J. Organomet. Chem.* **1994**, *465*, 85–92); Chan-Lam amination ((d) Vantourout, J. C.; Miras, H. N.; Isidro-Llobet, A.; Sproules, S.; Watson, A. J. B. *J. Am. Chem. Soc.* **2017**, *139*, 4769–4779); Liebskind-Srogl coupling ((e) Liebskind, L. S.; Srogl, J. J. *Am. Chem. Soc.*, **2000**, *122*, 11260–11261.); 1,4-addition to enones ((f) Sakai, M.; Hayashi, H.; Miyaura, N. *Organometallics*, **1997**, *16*, 4229–4231.); 1,2-addition to imines ((g) Sakai, M.; Ueda, M.; N. Miyaura, N. *Angew. Chem. Int. Ed.*, **1998**, *37*, 3279–3281).
- (4) Seiple, I. B.; Su, S.; Rodriguez, R. A.; Gianatassio, R.; Fujiwara, Y.; Sobel, A. L.; Baran, P. S. *J. Am. Chem. Soc.* **2010**, *132*, 13194–13196.
- (5) For a review on use of arylboronic acids as catalysts see: (a) Dimitrijević, E.; Taylor, M. S. *ACS Catal.* **2013**, *3*, 945–962. For applications see the following lead references. Amidation reactions: (b) Ishihara, K.; Ohara, S.; Yamamoto, H. *J. Org. Chem.*, **1996**, *61*, 4196–4197; (c) Ishihara, K.; Ohara, S.; Yamamoto, H. *Macromolecules*, **2000**, *33*, 3511–3513; (d) Ishihara, K.; Ohara, S.; Yamamoto, H. *Org. Synth.*, **2002**, *79*, 176–185; (e) Maki, T.; Ishihara, K.; Yamamoto, H. *Synlett*, **2004**, 1355–1358; (f) mechanistic studies, see: Al-Zoubi, R.M.; Marimon, O.; Hall, D. G. *Angew. Chem. Int. Ed.*, **2008**, *47*, 2876–2879. In Diels-Alder catalysis: (g) Zheng, H.; Hall, D. G. *Tetrahedron Lett.*, **2010**, *51*, 3561–3564; (h) Zheng, H.; Lejkowski, M.; Hall, D. G. *Tetrahedron Lett.*, **2013**, *54*, 91–94; (i) Zheng, H.; McDonald, R.; Hall, D. G., *Chem. Eur. J.*, **2010**, *16*, 5454–5460. In Friedel-Crafts reactions: (j) Ricardo, C. L.; Mo, X.; McCubbin, J. A.; Hall, D. G. *Chem. Eur. J.* **2015**, *21*, 4218–4223. (k) Liu, Y.-L.; Liu, L.; Wang, Y.-L.; Han, Y.-C.; Wang, D.; Chen, Y.-J. *Green Chem.*, **2008**, *10*, 635–640; (l) Sanz, R.; Martinez, A.; Miguel, D.; Alvarez-Gutiérrez, J. M.; Rodríguez, F. *Adv. Synth. Catal.*, **2006**, *348*, 1841–1845. In glycosylation reactions: (m) Nishi, N.; Nashida, J.; Kaji, E.; Takahashi, D.; Toshima, K. *Chem. Commun.* **2017**, *53*, 3018–3021; also using boronic acids: (n) D'Angelo, K. A.; Taylor, M. S. *J. Am. Chem. Soc.* **2016**, *138*, 11058–11066; (o) D'Angelo, K. A.; Taylor, M. S. *Chem. Commun.* **2017**, *53*, 5978–5980; In Nazarov cyclizations: (p) Zheng, H.; Lejkowski, M.; Hall, D. G. *Tetrahedron Lett.*, **2013**, *54*, 91–94; in [3+2] dipolar additions: (q) Zheng, H.; McDonald, R.; Hall, D. G. *Chem. Eur. J.*, **2010**, *16*, 5454–5460.
- (6) Kallepalli, V. A.; Gore, K. A.; Shi, F.; Sanchez, L.; Chotana, G. A.; Miller, S. L.; Maleczka, R. E., Jr.; Smith, M. R., III *J. Org. Chem.* **2015**, *80*, 8341–8353.
- (7) Ihara, H.; Sugimoto, M. *J. Am. Chem. Soc.*, **2009**, *131*, 7502–7503.
- (8) See, for example, the following reviews: (a) Brooks, W. L. A.; Vancoillie, G.; Kabb, C. P.; Hoogenboom, R.; Sumerlin, L. A.;

- B. S. J. *Polymer. Sci. A*. **2017**, 55, 2309–2317; (b) (a) Vancoilli, G.; Hoogenboom, R. *Sensors*, **2016**, 16, 1736; (c) Wu, X.; Chen, X.-X.; Jiang, Y.-B. *Analyst*, **2017**, 142, 1403–1414.
- (9) Vancoilli, G.; Hoogenboom, R. *Polymer Chem.*, **2016**, 7, 5484–5495.
- (10) Moy, C. L.; Kaliappan, R.; McNeil A. J. *J. Org. Chem.* **2011**, 76, 8501–8507.
- (11) Collins, J.; Nadgorny, M.; Xiao, Z.; Connal, L. A. *Macromol. Rapid. Commun.* **2017**, 38, 1600760.
- (12) Jacobson, O.; Kiesewetter D. O.; Chen, X. *Bioconjug. Chem.*, **2015**, 26, 1–18.
- (13) Wang, J.; Sánchez-Roselló, M.; Aceña, J. L.; Del Pozo, C.; Sorochinsky, A. E.; Fustero, S.; Soloshonok, V. A.; Liu, H. *Chem. Rev.* **2014**, 114, 2432–2506.
- (14) (a) Ainley, A. D.; Challenger, F. J. *Chem. Soc.* **1930**, 52, 2171–2180. (b) Kuivila, H. G.; Nahabedian, K. V. *J. Am. Chem. Soc.* **1961**, 83, 2159–2163. (c) Kuivila, H. G.; Nahabedian, K. V. *J. Am. Chem. Soc.* **1961**, 83, 2164–2166. (d) Nahabedian, K. V.; Kuivila, H. G. *J. Am. Chem. Soc.* **1961**, 83, 2167–2174. (e) Kuivila, H. G.; Reuwer, J. F.; Mangravite, J. A. *Can. J. Chem.* **1963**, 41, 3081–3090. (f) Kuivila, H. G.; Reuwer, J. F.; Mangravite, J. A. *J. Am. Chem. Soc.* **1964**, 86, 2164–2666. (g) Frohn, H. J.; Adonin, N. Y.; Bardin, V. V.; Starichenko, V. F. Z. *Anorg. Allg. Chem.* **2002**, 628, 2834–2838. (h) Cammidge, A. N.; Crépy, K. V. L. *J. Org. Chem.* **2003**, 68, 6832–6835. (i) Kinzel, T.; Zhang, Y.; Buchwald, S. L. *J. Am. Chem. Soc.* **2010**, 132, 14073–14075. (j) Lozada, J.; Liu, Z.; Perrin, D. M. *J. Org. Chem.* **2014**, 79, 5365–5368. (k) Adonin, N. Y.; Shabalin, A. Y.; Bardin, V. V. *J. Fluor. Chem.* **2014**, 168, 111–120. (l) Noonan, G.; Leach, A. G. *Org. Biomol. Chem.*, **2015**, 13, 2555–2560. (m) Cox, P. A.; Leach, A. G.; Campbell, A. D.; Lloyd-Jones, G. C. *J. Am. Chem. Soc.* **2016**, 138, 9145–9157.
- (15) For recent examples see: (a) Molloy, J. J.; Law, R. P.; Fyfe, J. W. B.; Seath, C. P.; Hirst, D. J.; Watson, A. J. B. *Org. Biomol. Chem.*, **2015**, 13, 3093–3102; and in polymer chemistry: (b) Schroot, R.; Schubert, U. S.; Jäger, M. *Macromolecules*, **2017**, 50, 1319–1330. (c) Ji, L.; Edkins, R. M.; Sewell, L. J.; Beeby, A.; Batsanov, A. S.; Fücke, K.; Drafcz, M.; Howard, J. A. K.; Moutounet, O.; Ibersiene, F.; Boucekkine, A.; Furet, E.; Liu, Z.; Halet, J.-F.; Katan, C.; Marder, T. B. *Chem. - Eur. J.* **2014**, 20, 13618–13635.
- (16) (a) Lee, C. Y.; Ahn, S. J.; Cheon, C. H. *J. Org. Chem.* **2013**, 78, 12154–12160; (b) Ahn, S.; Lee, C. Y.; Kim, N.; Cheon, C. *J. Org. Chem.*, **2014**, 79, 7277–7285; (c) Shen, F.; Tyagarajan, S.; Perera, D.; Krška S. W.; Maligres, P. E.; Smith, M. R., III; Maleczka, R. E., *Org. Lett.*, **2016**, 18, 1554–1557.
- (17) Hansen, M. M.; Jolly, R. A.; Linder, R. J. *Org. Process Res. Dev.*, **2015**, 19, 1507–1516.
- (18) See for example: (a) Liu, C.; Li, X.; Wu, Y.; Qiu, J.; *RSC Adv.*, **2014**, 4, 54307–54311; (b) Liu, C.; Li, X.; Wu, Y. *RSC Adv.*, **2015**, 5, 15354–15358; (c) Barker, G.; Webster, S.; Johnson, D. G.; Curley, R.; Andrews, M.; Young, P. C.; Macgregor, S. A.; Lee, A.-L. *J. Org. Chem.*, **2015**, 80, 9807–9816; (d) see reference⁶; (e) Zhang, G.; Li, Y.; Liu, J. *RSC Adv.*, **2017**, 5, 34959–34962; (f) for early studies, see reference^{14f}, and references therein.
- (19) K_a is the equilibrium constant for aqueous interconversion of $\text{ArB}(\text{OH})_2$ with $[\text{ArB}(\text{OH})_3]^- [\text{H}_3\text{O}]^+$; the equilibrium is pH controlled, with the mol-fraction boronic acid (x) and boronate (x_{OH}) being given by: $x_{\text{OH}} = 1/(1+10^{(\text{p}K_a-\text{pH})})$; and $x + x_{\text{OH}} = 1$. The hydroxide-control of this equilibrium is related by use of $K_{\text{OH}} = K_a/K_w$, where K_w is the autonation constant of water in the medium employed.
- (20) Data for "Kuivila" in Scheme 1 are taken from reference^{14e}. These data are from reactions conducted at 90 °C in malonate-buffered water at pH 6.7 (25 °C, uncorrected). The relative rates ($k_{\text{rel}(\text{est})}$) were calculated by extrapolation to reactions involving 100% boronate, using the $\text{p}K_a$ values estimated by Kuivila.
- (21) (a) Review: Tyrrell, E.; Brookes, P. *Synthesis* **2003**, 4, 469–483; see also: (b) Dick, G. R.; Woerly, E. M.; Burke, M. D. *Angew. Chem. Int. Ed.* **2012**, 51, 2667–2672; (c) Fuller, A. A.; Hester, H. R.; Salo, E. V.; Stevens, E. P. *Tetrahedron Lett.* **2003**, 44, 2935–2938; (d) Ishiyama, T.; Ishida, K.; Miyaura, N. *Tetrahedron* **2001**, 57, 9813–9816; (e) Fischer, F. C.; Havinga, E. *Recl. des Trav. Chim. des Pays-Bas* **1974**, 93, 21–24.
- (22) see for example (a) Kohlmann, J.; Braun, T.; Laubenstein, R.; Herrmann, R. *Chem. Eur. J.* **2017**, 23, in press, DOI: 10.1002/chem.201700549; (b) Korenaga, T.; Kosaki, T.; Fukumura, R.; Ema, T.; Sakai, T. *Org. Lett.* **2005**, 7, 4915–4917.
- (23) This issue highlights the problems associated with correlations that do not include mechanistically-rich *ortho*-substituents. For further discussion and solutions see: Santiago, C. B.; Milo, A.; Sigman, M. S. *J. Am. Chem. Soc.*, **2016**, 138, 13424–13430.
- (24) For full discussion of the mechanism of self/autocatalysis for 3-thienylboronic acid, see reference^{14m}.
- (25) This condition assumes that $\text{p}K_{\text{III}} > \text{p}K_w$, as is found for pyrazolyl- and 3,5-dimethyl-4-isoxazolyl boronates.^{14m}
- (26) $\text{B}(\text{OH})_3$ has a higher $\text{p}K_a$ (11.03 at 70 °C) than **24** (9.15 at 70 °C) resulting in the KOH acting catalytically when sub-stoichiometric. Such reactions evolve from pseudo zero-order to first order kinetics. Pure first order kinetics are obtained with stoichiometric and excess KOH. Use of maximum (initial) rate ($[\text{24}_{\text{OH}}]_0 \times k_{\text{PDB}}$; mM s⁻¹) allows direct comparison of all of the reactions, independent of KOH stoichiometry.
- (27) Gross, K. C.; Seybold, P. G.; Peralta-Inga, Z.; Murray, J. S.; Politzer, P. J. *Org. Chem.* **2001**, 66, 6919–6925.
- (28) Linear regression of $\log(k_X/k_H) = \rho^{\text{SL}}(\sigma^{\text{SL}} + n\sigma^{\text{o-F}})$ or $\log(K_{\text{aX}}/K_{\text{aH}}) = \rho^{\text{SL}}(\sigma^{\text{SL}} + n(\sigma^{\text{o-F}}))$ where ρ^{SL} and $\sigma^{\text{o-F}}$ are variables; $n = 0, 1$ or 2 (the number of *ortho* fluoro substituents).
- (29) Kono, Y.; Ishihara, K.; Nagasawa, A.; Umamoto, K.; Saito, K. *Inorg. Chim. Acta* **1997**, 262, 91–96.
- (30) The rather unlikely exception to this would be if the Brønsted / Lewis acid equilibrium constants (K_a and K_{aH}) are identical, in all cases.
- (31) (a) Yan, J.; Springsteen, G.; Deeter, S.; Wang, B. *Tetrahedron* **2004**, 60, 11205–11209; (b) Branch, Y. E. K.; Yabroff, D. L.; Bettman, B. *J. Am. Chem. Soc.* **1934**, 56, 937–941.
- (32) $\text{Mo6L}/6\text{-}311++\text{G}^{**}$, incorporating solvation free energies computed as single points employing the same level of theory and the PCM formalism.³³ Solvation was incorporated using PCM settings for methanol as a solvent with polarity intermediate between water and dioxane. This level gave best quantitative agreement with experiment for MIDA hydrolysis.^{2b} Calculations were performed in Gaussian09³⁴ at 298 K/1 atm, or for KIEs at 343K, 1M.
- (33) (a) Zhao, Y.; Truhlar, D. G. *Acc. Chem. Res.* **2008**, 41, 157–167. (b) Zhao, Y.; Truhlar, D. G. *Theor. Chem. Acc.* **2008**, 120, 215–241. (c) Tomasi, J.; Mennucci, B.; Cammi, R. *Chem. Rev.* **2005**, 105, 2999–3094.
- (34) See SI for full citations: Frisch, M. J.; *et al.* Gaussian 09, Revision C.01; Gaussian, Inc.: Wallingford, CT, 2009.
- (35) Wigner, E. *Phys. Rev.* **1932**, 40, 749–759.
- (36) Aziz, H. R.; Singleton, D. A. *J. Am. Chem. Soc.* **2017**, 139, 5965–5972.

(37) For discussion and leading references on the ionic radius of the solvated hydroxonium ion, see: Iyengar, S. S.; Petersen, M. K.; Day, T. J. F.; Burnham, C. J.; Teige, V. E.; Voth, G. A. *J. Chem. Phys.* **2005**, *123*, 084309.

(38) Cammidge, A. N.; Goddard, V. H. M.; Gopee, H.; Harrison, N. L.; Hughes, D. L.; Schubert, C. J.; Sutton, B. M.; Watts, G. L.; Whitehead, A. J. *Org. Lett.* **2006**, *8*, 4071–4074.

(39) Control experiments / rapid pH-quenching confirmed that the observed partitioning factors were not a result of, or affected by, post-protodeboronation exchange of Ar-L with L_2O / OL^- .

(40) Perrin, C. L.; Reyes-Rodríguez, G. J. *J. Am. Chem. Soc.*, **2014**, *136*, 15263–15269.

(41) (a) Kwan, E. E.; Park, Y.; Besser, H. A.; Anderson, T. L.; Jacobsen, E. N. *J. Am. Chem. Soc.*, **2017**, *139*, 43–46; (b) Singleton, D. A.; Thomas, A. A. *J. Am. Chem. Soc.*, **1995**, *117*, 9357–9358.

(42) An analogous equilibrium isotope effect (EIE) causes isotopic fractionation of $B(OH)_3$ and $[B(OH)_4]^-$ in seawater ($K_{10B}/K_{11B} \geq 1.03$) making this a useful paleo-pH proxy, see Zeebe, R. E. *Geochim. Cosmochim. Acta*, **2005**, *69*, 2753–2766.

(43) (a) Perrin, C. L.; Dong, Y. *J. Am. Chem. Soc.* **2007**, *129*, 4490–4497.

(44) Benzyne have been generated from phenylboronates bearing ortho-nucleofuges under *anhydrous conditions*, see for example: (a) Verbit, L.; Levy, J. S.; Rabitz, H.; Kwalwasser, W. *Tetrahedron Lett.* **1966**, *7*, 1053–1055. Photochemical deboronation / benzyne generation has also been reported: (b) Fischer, F. C.; Havinga, E. *Recl. des Trav. Chim. des Pays-Bas* **1974**, *93*, 21–24. Benzyne-generation from *ortho*-anionic aryltriflates appears to be accelerated when arylmetallation occurs: (c) Dyke, A. M.; Gill, D. M.; Harvey, J. N.; Hester, A. J.; Lloyd-Jones, G. C.; Munoz, M. P.; Shepperson, I. R. *Angew. Chem. Int. Ed.* **2008**, *47*, 5067–5070.

(45) Wiberg, K.B. *Tetrahedron* **1968**, *24*, 1083–1096

(46) For a LFER and KIE study on the generation of arylanions by decarboxylation of arylcarboxylates, see: (a) Segura, P.; Bunnett, J. F.; Villanova, L. *J. Org. Chem.* **1985**, *50*,

1041–1045; and (b) Segura, P.; *J. Org. Chem.* **1985**, *50*, 1046–1053. For a recent methodology involving the opposite process: an aryl anion reacting with boron to generate an Ar-B product, see: (c) Lee, Y.; Baek, S.-y. Park, J.; Kim, S.-T.; Tussupbayev, S.; Kim, J.; Baik, M.-H.; Cho, S. H. ; *J. Am. Chem. Soc.*, **2017**, *139*, 976–984. We also note that exposure of pentafluorobenzene **30_H** (the product of protodeboronation of **30**) to 70°C dioxane/ L_2O , at pH(D) >13, for >100 msec results in detectable H/D exchange at C-H; presumably via **30_{anion}**.

(47) (a) Reed, A.E.; Weinstock, R.B.; Weinhold, F. *J. Chem. Phys.* **1985**, *83*, 735–746; (b) Reed A. E.; Weinhold, F. *J. Chem. Phys.* **1985**, *83*, 1736–1740.

(48) In a later work^{14f} discussing the mechanism of Cd-catalysis, Kuivila suggested that the correlation of the rate of base-catalyzed protodeboronation with σ , rather than σ^+ , suggested an SE₂ mechanism. This change in interpretation from that originally presented^{14e} appears to have been stimulated by discussion with Traylor: Minatot, H.; Ware, J. C.; Traylor T. G. *J. Am. Chem. Soc.* **1963**, *85*, 3024–3026.

(49) Kuivila also evaluated the impact of *ortho*-substitution using Taft *o/p* rate-factors. However, combinations of steric / electrostatic effects were proposed to account for the rate acceleration via pathway I_A.

(50) The rapid decomposition of **30/30_{OH}** makes pK_a determination technically challenging, see for example: Yamamoto, Y.; Matsumura, T.; Takao, N.; Yamagishi, H.; Takahashi, M.; Iwatsuki, S.; Ishihara, K. *Inorg. Chim. Acta* **2005**, *358*, 3355–3361.

(51) For examples where pentafluorophenylboronic acid (**30**), and its ester derivatives, is stable under anhydrous reactions conditions, even with prolonged heating (150 °C) see: (a) Hofer, M.; Gomez-Bengoa, E.; Nevado, C. *Organometallics* **2014**, *33*, 1328–1332; (b) Hofer, M.; Genoux, A.; Kumar, R.; Nevado, C. *Angew. Chem. Int. Ed.* **2017**, *56*, 1021–1025.

GRAPHICAL ABSTRACT

